

Synthesis and Characterization of Cu Nanoparticle Using High Energy Ball Milling Route and Compare with Scherrer Equation

Rajeshkanna .S¹, Nirmalkumar .O²

¹PG Scholar, Department of Product Design and Development, Sona College of Technology, Tamilnadu, India

²PG Scholar, Department of Product Design and Development, Sona College of Technology, Tamilnadu, India

Abstract: This proposed work is to produce Mechanical alloying materials from a variety of materials such as copper powder spherical -100 mesh, 99% metal basis through High Energy Ball milling. Nano crystalline copper powder was produced by ball milling of copper powder spherical -100 mesh, 99% metal basis the powder samples have been taken by HEBM 30hrs, 45hrs and 75hrs at constant speed of 250rpm with BPR 10:1. Characterization and phase of copper Nano materials investigated by using X-ray diffraction. And also to develop and prediction of new Nano copper based material through mechanical alloying by High energy ball milling route and also determine the crystalline size of cu particle used Scherrer Equation.

Keywords: High Energy Ball milling, Nano crystalline copper powder, X-ray diffraction Scherrer Equation.

1. Introduction

In recent years research involving nanoparticles and nanoscale materials has generated a great deal of interest from scientists and engineers of nearly all disciplines. Experiments were conducted at LMW-CNC-LAL-2 production lathe using PCD 1500 grade insert at various cutting conditions and parameters such as surface roughness, specific power consumed, and tool wear were measured [1]. In fact, at least one colloidal copper manufacturer has been cited for violating the Pure Food and Drug Act for citing health benefits in his advertisements [4]. In addition, nanosized copper particles are currently sold for application in polymers and plastics, lubricants, inks and metallic coatings. The tool life data have been analyzed using regression techniques and a general form of the Taylor equation has been developed to describe the tool performance on this composite [2]. A maximum magnetostrictive susceptibility of 930 ppmT⁻¹ at a field of $\mu_0 H = 0.1$ T was obtained. The hardness varied from 150 HV10 to 340 HV10 with increasing amount of the amorphous phase [9]. develop and prediction of new nano copper based material through mechanical alloying by High energy ball milling route.

2. Experimental Details

The alloying process can be carried out using different apparatus, namely, attritor, planetary mill or a horizontal ball mill. However, the principles of these operations are same for all the techniques. Since the powders are cold welded and fractured during mechanical alloying, it is critical to establish a balance between the two processes in order to alloy successfully. Planetary ball mill is a most frequently used system for mechanical alloying since only a very small amount of powder is required. Therefore, the system is particularly suitable for research purpose in the laboratory. The ball mill system consists of one turn disc (turn table) and two or four bowls. The turn disc rotates in one direction while the bowls rotate in the opposite

direction. The centrifugal forces, created by the rotation of the bowl around its own axis together with the rotation of the turn disc, are applied to the powder mixture and milling balls in the bowl. The powder mixture is fractured and cold welded under high energy impact.

The figure below shows the motions of the balls and the powder. Since the rotation directions of the bowl and turn disc are opposite, the centrifugal forces are alternately synchronized. Thus friction resulted from the hardened milling balls and the powder mixture being ground alternately rolling on the inner wall of the bowl and striking the opposite wall. The impact energy of the milling balls in the normal direction attains a value of up to 40 times higher than that due to gravitational acceleration. Hence, the planetary ball mill can be used for high-speed milling.

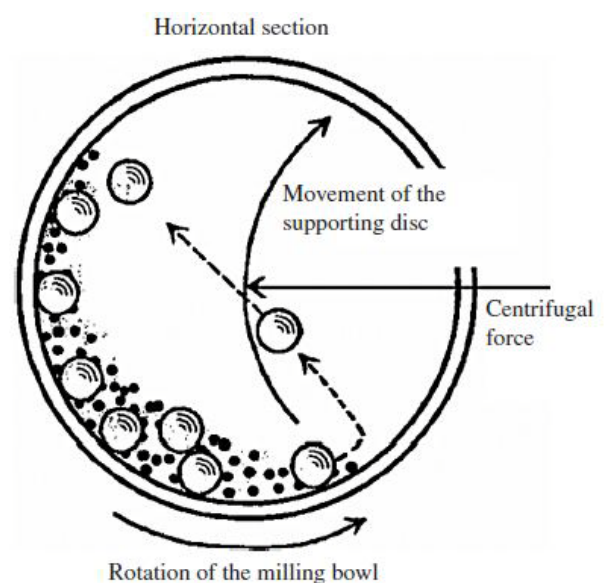


Figure 1: Schematic view of motion of the ball and powder mixture

During the high-energy ball milling process, the powder particles are subjected to high energetic impact. Microstructurally, the mechanical alloying process can be divided into four stages: (a) initial stage, (b) intermediate stage, (c) final stage, and (d) completion stage.

- (a) At the initial stage of ball milling, the powder particles are flattened by the compressive forces due to the collision of the balls. Micro-forging leads to changes in the shapes of individual particles, or cluster of particles being impacted repeatedly by the milling balls with high kinetic energy. However, such deformation of the powders shows no net change in mass.
- (b) At the intermediate stage of the mechanical alloying process, significant changes occur in comparison with those in the initial stage. Cold welding is now significant. The intimate mixture of the powder constituents decreases the diffusion distance to the micrometer range. Fracturing and cold welding are the dominant milling processes at this stage. Although some dissolution may take place, the chemical composition of the alloyed powder is still not homogeneous.
- (c) At the final stage of the mechanical alloying process, considerable refinement and reduction in particle size is evident. The microstructure of the particle also appears to be more homogenous in microscopic scale than those at the initial and intermediate stages. True alloys may have already been formed.
- (d) At the completion stage of the mechanical alloying process, the powder particles possess an extremely deformed metastable structure. At this stage, the lamellae are no longer resolvable by optical microscopy. Further mechanical alloying beyond this stage cannot physically improve the dispersed distribution. Real alloy with composition similar to the starting constituents is thus formed.

Theoretical considerations and explorations of planetary milling process have been broadly studied in order to better understand and integrate the concept. Joisel's work is the first report to study the shock kinematics of a "satellite milling machine." This work focused on the determination of the milling parameters that were optimized for shock energy. The various parameters were determined geometrically and the theoretical predictions were examined experimentally using a specifically designed planetary mill. Schilz et al. reported that from a macroscopical point of view, the geometry of the mill and the ratio of angular velocities of the planetary to the system wheel played crucial roles in the milling performance. For a particular ductile-brittle Mg-Si system, the milling efficiency of the planetary ball was found to be heavily influenced by the ratio of the angular velocity of the planetary wheel to that of the system wheel as well as the amount of sample load. Mio et al. studied the effect of rotational direction and rotation-to-revolution speed ratio in planetary ball milling. Some more theoretical issues and kinematic modeling of the planetary ball mill were reported later in related references. Because mechanical alloying of materials are complex processes which depend on many factors, for instance on physical and chemical parameters such as the precise dynamical conditions, temperature, nature of the grinding atmosphere, chemical

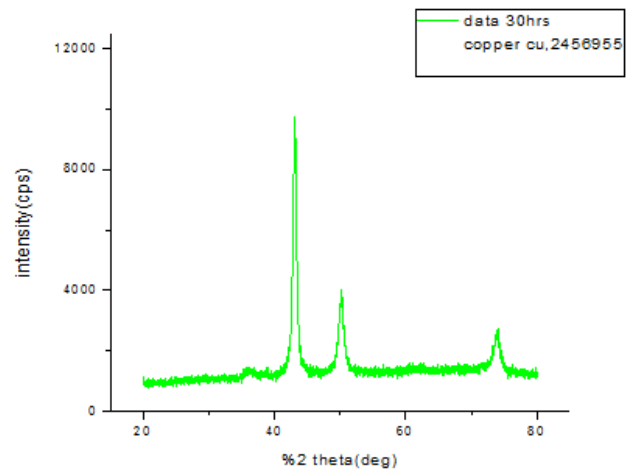
composition of the powder mixtures, chemical nature of the grinding tools, etc., some theoretical problems, like predicting equilibrium phase transitions under milling, are still in debate.

3. Results

The aim & objective of this proposed work is to produce Mechanical alloying materials from a variety of materials such as copper powder and Cu alloy and calculate the crystalline size of cu particles by using Scherrer Equation. BM was carried out using a high-energy Fritsch Pulverisette P-7 planetary planetary mill with cemented carbide balls as the milling media. The powder samples have been taken by HEBM 30hrs, 45hrs and 75hr at constant speed of 250rpm with The ball to powder mass ratio is (BPR) 10:1 The rotation speed of its vials (anticlockwise rotation) which are fixed onto a rotating disk and the rotation speed of disk (clockwise rotation) can be set independently. Characterization and phase of copper nano materials investigated by using X-ray diffraction(XRD). The XRD patterns of powders produced under conditions 250/30h, 250/45 and 250/75 corresponding to three different power values. XRD analyses were performed with a Rigaku high resolution diffractometer. Table 1 shows measuring condition for all cu powders (30hrs, 45hrs, 75hrs). Figure 2 shows fragments of XRD peaks experimentally obtained for 30hrs, 45hrs, 75hrs. Figure 3. shows Crystal Structure Of Copper-30hrs, 45hrs, 75hrs.

Table 1: Measurement Conditions

X-Ray	30 kV , 100 mA	Scan speed / Duration time	4.0000 deg/min
Goniometer	SmartLab	Step width	0.0200
Attachment	Standard	Scan axis	Theta/2-
Filter	Cu_K-beta	Scan range	20.0000 - 80.0000
CBO	BB	Incident slit	2/3deg
Diffracted	None	Length	10.0mm
Detector	SC-70	Receiving	2/3deg
Scan mode	CONTINUOUS	Receiving	0.150mm



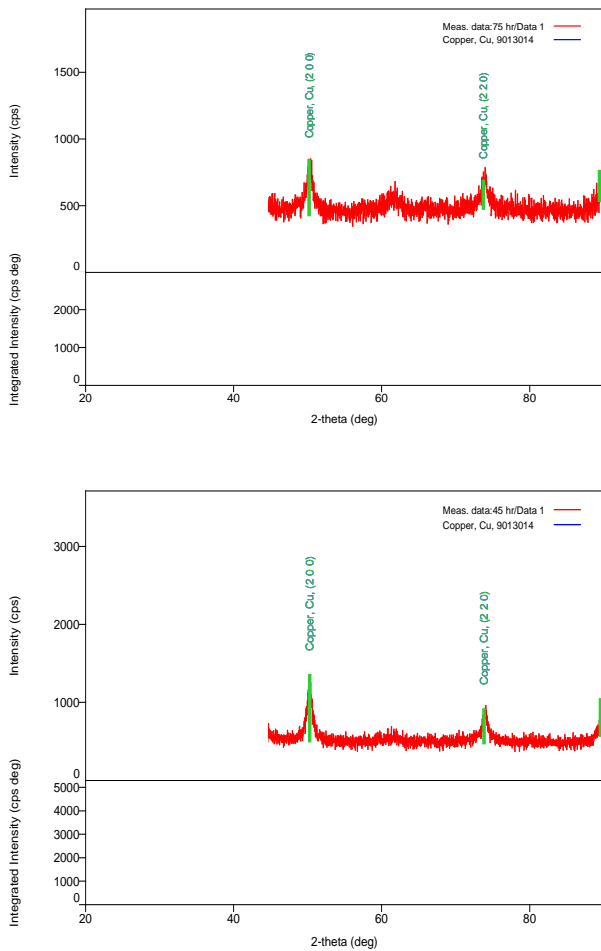


Figure 2: XRD patterns of all-milled powder during 30hrs, 45hrs, 75hrs

Peak values of XRD for 30 hrs and 250 rpm are given the table 2 with theta values and height of the peak then Asym. Factor, FWHM (deg), Int. I(cps deg), Int. W(deg). Peak values of XRD for 45 hrs and 250 rpm are given the table 3 with theta values and height of the peak then Asym. Factor, FWHM (deg), Int. I(cps deg), Int. W(deg). Peak values of XRD for 75 hrs and 250 rpm are given the table 4 with theta values and height of the peak then Asym. factor, FWHM(deg), Int. I(cps deg), Int. W(deg).

Peak List for 30 hrs

Table 2: Peak List for 250/30hr

No.	2-theta(deg)	d(ang.)	Height(cps)	FWHM(deg)	Int. I(cps deg)	Int. W(deg)	Asym. factor
1	43.16 (1)	2.0964(5)	3333.33(90)	0.342(12)	1456(15)	0.55(3)	1.00(10)
2	50.02 (2)	1.8162(8)	617(45)	0.84(3)	521(11)	0.85(8)	0.76(11)
3	73.94 (3)	1.2816(4)	412(32)	0.72(5)	324(7)	1.04(13)	1.1(3)

Scherrer Equation

The Scherrer equation, in X-ray diffraction and crystallography, is a formula that relates the size of sub-micrometre particles, or crystallites, in a solid to the broadening of a peak in a diffraction pattern. It is named after Paul Scherrer. It is used in the determination of size of particles of crystals in the form of powder.

The Scherrer equation can be written as:

$$\tau = \frac{K\lambda}{\beta \cos \theta}$$

Where:

- τ is the mean size of the ordered (crystalline) domains, which may be smaller or equal to the grain size;
- K is a dimensionless shape factor, with a value close to unity. The shape factor has a typical value of about 0.9, but varies with the actual shape of the crystallite;
- λ is the X-ray wavelength;
- β is the line broadening at half the maximum intensity (FWHM), after subtracting the instrumental line broadening, in radians. This quantity is also sometimes denoted as $\Delta(2\theta)$;

Crystalline Size Calculation:

Scherrer Equation

Peak value 1

$$\tau = \frac{K\lambda}{\beta \cos \theta}$$

$K = 0.9$

$$= \frac{0.9 \times 0.15418}{0.342 \times 0.9299}$$

Peak value 2

$$= \frac{0.9 \times 0.15418}{0.83 \times 0.9062}$$

Peak value 3

$$= \frac{0.9 \times 0.15418}{0.72 \times 0.7989}$$

$= 0.2411 \text{ nm}$

Crystalline size (D):

$$D = \frac{0.318027 + 0.1844 + 0.2411}{3}$$

$= 0.2478 \text{ nm}$

Peak List for 45 hrs:

Table 3: Peak List for 250/45hr

No.	2-theta(deg)	d(ang.)	Height(cps)	FWHM(deg)	Int. I(cps deg)	Int. W(deg)	Asym. Factor
1	43.1	2.09	1872(0.470(148	0.7	1.1
2	50.2	1.81	456(3	0.84(3	555(1.2	0.9
3	73.9	1.28	275(3	0.73(9	377(1.3	0.9(

Crystalline size calculation for 45 hrs:

Scherrer Equation

Peak value 1

$$\tau = \frac{K\lambda}{\beta \cos \theta}$$

K = 0.9

$$= \frac{0.9 \times 0.15418}{0.470 \times 0.9287}$$

= 0.3179 nm

Peak value 2

$$= \frac{0.9 \times 0.15418}{0.84 \times 0.9054}$$

= 0.1823 nm

Peak value 3

$$= \frac{0.9 \times 0.15418}{0.73 \times 0.7990}$$

= 0.2377 nm

crystalline size(D):

$$D = \frac{0.3179 + 0.1823 + 0.2377}{3}$$

D = 0.2459 nm

Peak List for 75 hrs:

Table 4: Peak List for 250/75hr

No.	2-theta(deg)	d(ang.)	Height(cps)	FWHM(deg)	Int. I(cps deg)	Int. W(deg)	Asym. Factor
1	43.15	2.094	1872	0.470	1486	0.79	1.18
2	50.22	1.815	456	0.84	555	1.22	0.94
3	73.92	1.281	275	0.73	377	1.37	0.9

Crystalline size calculation for 75 hrs:

Scherrer Equation

Peak value 1

$$\tau = \frac{K\lambda}{\beta \cos \theta}$$

K = 0.9

$$= \frac{0.9 \times 0.15418}{0.470 \times 0.9299}$$

= 0.3173 nm

Peak value 2

$$= \frac{0.9 \times 0.15418}{0.84 \times 0.9055}$$

= 0.1823 nm

Peak value 3

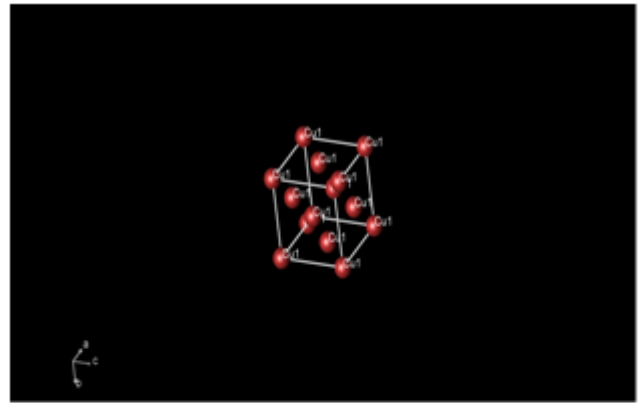
$$= \frac{0.9 \times 0.15418}{0.73 \times 0.7990}$$

= 0.2377 nm

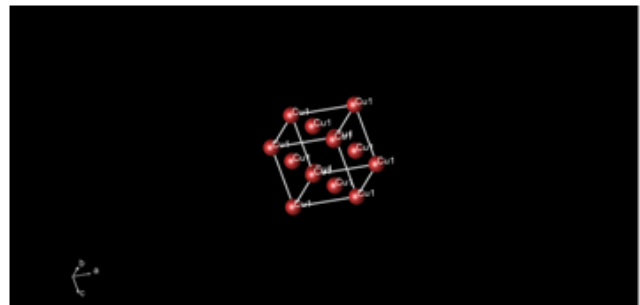
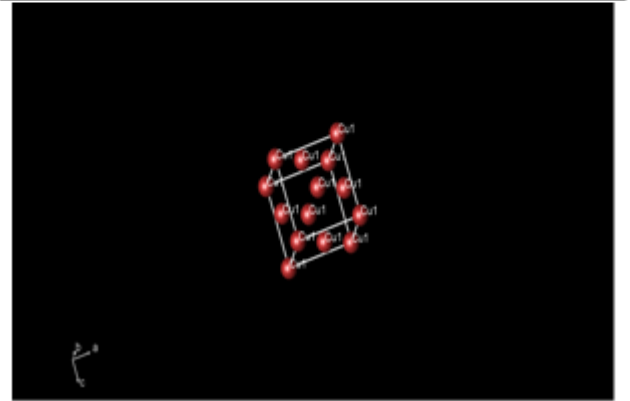
crystalline size(D):

$$D = \frac{0.3173 + 0.1823 + 0.2377}{3}$$

= 0.2457 nm



Crystal Structure of Copper-30 Hrs Crystal Structure of Copper-45 Hrs



Crystal Structure of Copper-75 Hrs

Figure 3: Crystal Structure of Copper-30hrs, 45hrs, 75 hrs.

Figure 3 shows the Crystal Structure of Copper powder samples in different stages, in contrast, the case with same BPR-same rpm and different BM hours revealed a totally different crystal structures evolution. Figure 4, 5, 6 shows the microstructure evolution of the samples in different stages, BM conditions of BPR 10:1, 250 rpm for 25hr, BPR 10:1, 250 rpm for 45 hr, and BPR 10:1, 250 rpm for 75 hr, respectively. The case of revealed similar microstructures evolution with that of same BPR, same rpm and different hr. For evolution of microstructure of the samples in different stages used Olympus metallurgical microscope with CMOS camera. Make : Olympus, Japan Optical system : Universal Infinity System, Focusing system full stroke : 25mm Magnification (maximum) : 1500X, Resolution : 1.3-Megapixel, 1280 x 1024 pixels, Pixel pitch : 5.2µm x 5.2µm.

4. Microstructures Observation of Cu Particles



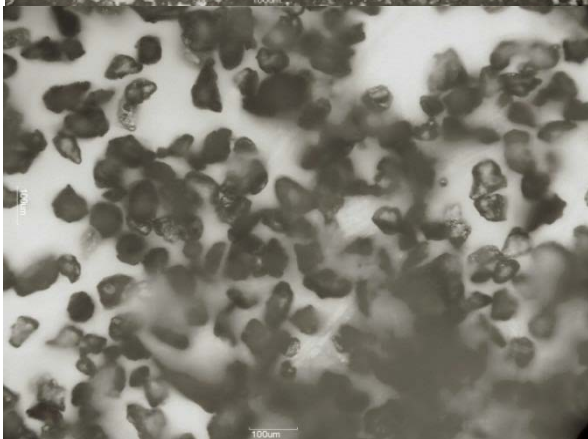
100um(a),150x100um(b),300x

Figure 4: microstructures observation: (a),(b) the samples with BPR 10:1 and 250 rpm30hrs



100um(a),150x 100um(b),300x

Figure 6: microstructures observation: (a), (b) the samples with BPR 10:1 and 250 rpm45hrs



100um(a),150x100um(b),300x

Figure 5: microstructures observation: (a),(b) the samples with BPR 10:1 and 250 rpm45hrs

Figure 4a,b. In contrast, the case with 10:1 BPR-250 rpm and 30hrs revealed a totally different microstructure (100um, 150x, 300x.) evolution from Figure 5. Figure 5a,b. In contrast, the case with 10:1 BPR-250 rpm and 45hr revealed a totally microstructure (100um, 150x, 300x.) evolution from Figure 6. Figure 6a,b. In contrast, the case with 10:1 BPR-250 rpm and 75hrs revealed a totally microstructure (100um, 150x, 300x.) evolution from Figure 4, 5.

XRD peaks 30hrs value is 2.11ang and nano size 200nm,45hrs value is 2.09 and nano size 100nm and 75hr value is 2.01 and nano value 100nm, finally peaks have been decreases so 75hrs is the better nano material stage based on the above results.

5. Conclusion

The various synthesis processes of nano powder and journal related to mechanical alloying process are studied, based on the literature support copper and copper alloys identified. In this proposed work a systematic view of the basic concept of mechanical milling, historical view and applications of mechanical milling in the synthesis of various copper nano materials and various structures have been studied.

Peak values calculated by XRD and compared Scherrer formula. In this above table2 indicates first peak value is high, table3 indicates second value low and table4



indicates third value very low when compared to other 2 peak values. Then XRD peaks 30hrs value is 0.2478avg and nano size 100nm, 45hr value is 0.2459avg and nano size 100nm and 75hr value is 0.2457 avg and nano value 100nm, finally peaks have been decreases so 75hr is the better nano material stage based on the above results.

In future to develop a novel copper alloy metal matrix composite alloy through mechanical alloying by high energy ball milling route.

This results show that Scherrer equation is an easy way to evaluate the mean diameter in nano-sized copper particle cases. In some particular cases copper material this relation must be completed with other theory that take in account lattice site of crystalline structure. Otherwise, this equation can be the first evaluation of mean diameter distribution. Then conclude directly XRD pattern, if large rings appear than samples in study has a low values for mean diameter than in case if thick rings appear.

References

- [1] Brouisol. British Patent No. 392556, 1931.
- [2] Canano Technologies, 230 Metcalf Street, P.O. Box 911, Tweed, Ontario, K0K 3J0.
- [3] Dresher, W. H., "Speeding up your computer in the 21st Century using Copper ICs," Innovations, Copper Development Association Inc., January 2000.
- [4] Farzana Hussain, Mehdi Hojjati, Masami Okamoto, Russell e. gorga "Review article: Polymer-matrix Nanocomposites, Processing, Manufacturing, and Application: An Overview" Journal of Composite Materials 2006; 40; 1511 DOI: 10.1177/0021998306067321
- [5] J.T. Lin D. Bhattacharyya, C. Lane "Machinability of a silicon carbide reinforced aluminium metal matrix composite" Wear 181-183 (1995) 883-888
- [6] N.Muthukrishnan & M. Murugan & K. Prahlada Rao "Machinability issues in turning of Al-SiC (10p) metal matrix composites" Int J Adv Manuf Technol (2008) 39:211
- [7] Mahamani.A "Machinability Study of Al-5Cu-TiB2 In-situ Metal Matrix Composites Fabricated by Flux-assisted Synthesis" Journal of Minerals & Materials Characterization & Engineering jmmce.org, Vol. 10, No.13, pp.1243-1254, 2011
- [8] N. Muthukrishnan & M. Murugan & K. Prahlada Rao "An investigation on the machinability of Al-SiC metal matrix composites using PCD inserts" Int J Adv Manuf Technol (2008) 38:447-454 DOI 10.1007/s00170-007-1111-z.
- [9] Sujit Das, R. Behera, G. Majumdar, B. Oraon, G. Sutradhar " An experimental investigation on the machinability of powder formed silicon carbide particle reinforced aluminium metal matrix composites" International Journal of Scientific & Engineering Research Volume 2, Issue 7, July-2011 1 ISSN 2229-5518
- [10] R.Venkatesh, A.M.Hariharan, N.Muthukrishnan "Machinability Studies of Al/SiC/ (20p) MMC by Using PCD Insert (1300 grade)" Proceedings of the